Primljen / Received: 18.11.2018.
Ispravljen / Corrected: 25.3.2019.
Prihvaćen / Accepted: 25.4.2019.
Dostupno online / Available online: 10.8.2019.

Buckling resistance of stainless steel angle column

Authors:

[1]**Aljoša Filipović**, MCE
afilipovic@grf.bg.ac.rs

[1]Assoc.Prof. **Jelena Dobrić**
jelena@imk.grf.bg.ac.rs

[1]Prof. **Zlatko Marković**
zlatko@imk.grf.bg.ac.rs

[2]**Nancy Baddoo**, MSc. CE
n.baddoo@steel-sci.com

[3]**Željko Flajs** , MSc. CE
zeljko.flajs@institutims.rs

[1]University of Beograd, Serbia
Faculty of Civil Engineering

[2]Steel Construction Institute, United Kingdom

[3]Institute for Testing of Materials Belgrade, Serbia

Preliminary note

Aljoša Filipović, Jelena Dobrić, Zlatko Marković, Nancy Baddoo, Željko Flajs

Buckling resistance of stainless steel angle columns

A numerical study of compressive capacities of stainless steel angle columns is presented in the paper in order to assess the design procedures presented in Eurocode 3. The study focuses on pin-ended hot-rolled equal angle columns made of austenitic stainless steel grade EN 1.4301. The study shows that the implementation of buckling curve b, used for the design of carbon steel hot-rolled angles, gives higher and unsafe buckling resistance of equivalent stainless steel angles in low and intermediate slenderness domains in comparison with numerical results.

Key words:
stainless steel, angle column, buckling, finite element analysis, Eurocode 3

Prethodno priopćenje

Aljoša Filipović, Jelena Dobrić, Zlatko Marković, Nancy Baddoo, Željko Flajs

Otpornost na izvijanje tlačnih elemenata izvedenih kutnicima od nehrđajućeg čelika

U radu je prikazano numeričko istraživanje tlačnog kapaciteta elemenata izvedenih kutnicima od nehrđajućeg čelika kako bi se procijenili postupci projektiranja navedeni u Eurokodu 3. Istraživanje je usmjereno na tlačne elemente izvedene kutnicima jednakih krakova sa zglobnim spojevima na kraju, u kvaliteti austenitnog nehrđajućeg čelika EN 1.4301. Utvrđeno je da primjena krivulje izvijanja b, koja se koristi za projektiranje tlačnih elemenata izvedenih kutnicima od toplo valjanog ugljičnog čelika, daje veću i otpornost na izvijanje koja nije na strani sigurnosti u slučaju ekvivalentnih tlačnih elemenata izvedenih kutnicima od nehrđajućeg čelika u područjima niske i srednje vitkosti u usporedbi s numeričkim rezultatima.

Ključne riječi:
nehrđajući čelik, tlačni element izveden kutnikom, izvijanje, analiza konačnih elemenata, Eurokod 3

Vorherige Mitteilung

Aljoša Filipović, Jelena Dobrić, Zlatko Marković, Nancy Baddoo, Željko Flajs

Biegefestigkeit von Druckelementen aus Edelstahlwinkeln

Die Arbeit enthält eine numerische Studie zum Druckvermögen von Elementen aus Edelstahlwinkeln, um die in Eurocode 3 festgelegten Entwurfsverfahren zu bewerten. Die Forschung konzentriert sich auf Druckelemente, die aus gleichschenkligen Winkeln mit Gelenkverbindungen am Ende in der Qualität des austenitischen rostfreien Stahls EN 1.4301 hergestellt werden. Es hat sich gezeigt, dass die Anwendung der Biegekurve b, die für die Auslegung von Druckelementen aus warmgewalztem Kohlenstoffstahl verwendet wird, bei gleichwertigen Druckelementen aus Edelstahlwinkeln in Bereichen mit geringer und mittlerer Stärke eine höhere und nicht sicherheitsrelevante Biegefestigkeit im Vergleich zu numerischen Ergebnissen ergibt.

Schlüsselwörter:
Edelstahl, Druckelement aus Winkeln, Verbiegung, Analyse fertiger Elemente, Eurocode 3

1. Introduction

1.1. Background

Single-angle members exposed to compression have typically been used in civil engineering as members of trusses, latticed transmission towers, communication structures, or built-up columns. If these structures are situated in aggressive or urban environments, numerous stainless steel alloys may be beneficially utilized due to their corrosion resistance, attractive appearance, low maintenance requirements, good strength, toughness and fatigue properties.

Stainless steel structural sections (e.g. I-shaped members, angles, channels, tees, rectangular hollow sections) can be produced by cold forming, hot rolling, extrusion, and arc or laser welding. Stainless steel hot rolled angles are available in sizes of up to approximately 150 mm in leg length. Larger angles are made by cold forming or welding.

Even though the geometry of an angle section is simple, its asymmetry and non-coincidence of the shear centre (*S*) with the section's centroid (*G*) may lead to complex determination of the compressive capacity of angle columns (see Figure 1). The position of shear centre at the intersection of angle legs produces a negligible warping torsional stiffness. Thus, depending on material properties, cross-section slenderness, overall slenderness, and boundary conditions, the failure of the centrically compressed angle member occurs due to flexural buckling about the minor principal axis of the cross-section, or flexural–torsional buckling. Furthermore, angle columns are usually connected at their ends through one leg, which introduces eccentricities related to the section's centroid and leads to biaxial flexural deformations that consequently affect their ultimate structural response.

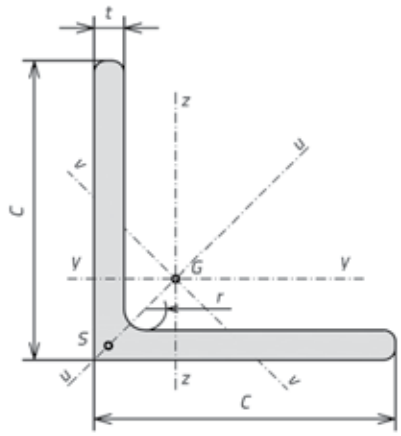

Figure 1. Designations of equal angle section

The design of centrically compressed stainless steel angle members is not currently covered by any European codified procedure. The lack of experimental data in this structural field has resulted in the current design provisions in EN 1993-1-4 [1] relying solely on assumed analogies with equivalent carbon steel members. Clause 5.4.1 [1] allows the use of appropriate provisions given in EN 1993-1-1 [2] and EN 1993-1-3 [3] for the design of compressed stainless steels members but with modifications given in clause 5.4.2 [1]. However, the analytical method in clause 5.4.2 does not explicitly state the values of neither the imperfection factor nor the limiting slenderness for stainless steel angles in the relevant buckling plane, depending both on the manufacturing process and steel grade. Exceptions to this rule are generally designated cold-formed open sections. However, it should be noted that when these rules were developed, there were no data on hot rolled angles nor on cold formed angles. Thus, this kind of approach can lead to misconceived design practice since it does not offer a clear response to the important issue related to the application of corresponding design curves for a reliable and safe prediction of buckling resistance of compressed stainless steel angle members.

Single angles loaded through one leg fail by interaction between the axial force and biaxial bending The design procedure stated in Annex BB of EN 1993-1-1 [2] treats this interaction by adopting a non-dimensional effective (modified) slenderness ratio instead of a geometrical one, under the condition that both ends of the column are welded or connected by at least two bolts. This procedure accounts for both the eccentricities and restraints at the member's ends.

Unlike carbon steel, stainless steel has a predominantly nonlinear stress–strain relationship without a clearly defined yield strength and with significant strain hardening and ductility. The gradual yielding between the low proportionality stress and yield strength leads to a softening of the material and consequently affects structural response of stainless steel elements. Hence, the design buckling curves for stainless steel columns may differ in comparison with equivalent carbon steel columns.

This paper presents the initial phase of an ongoing investigation that is performed at the University of Belgrade, Faculty of Civil Engineering. This paper addresses stainless steel columns with single hot-rolled equal angle sections centrically subjected to compression. An experimental programme that covers standard material tensile tests and a Finite Element (FE) study of column buckling behaviour are presented. The obtained numerical results are used to assess accuracy of the calculation method for the design of compressed angle members according to existing European specifications [1, 2].

1.2. State of the art

Significant experimental and analytical research on the behaviour of compressed carbon steel angle members

has been conducted in the past decades to develop comprehensive design guidelines with a wide range of fabricated products and material properties including both mild and high-strength steel materials. Observations made with regard to carbon steel angle columns may serve as a basis for better understanding of the structural behaviour of equivalent columns made of stainless steel. Such results are useful for quantifying the effects of geometric imperfections, end eccentricity or end restraint on SS angle column strength. The first experimental study of the load compression capacity of angles was conducted by Stang and Strlckenberg [4] in 1924. The authors tested a series of 170 standard rolled steel angles with different end connections, such as square, bolted, and flat-ended bolted. Wakabayashi and Nonaka [5] (1965) carried out an experimental investigation on 57 hot-rolled angles in which they varied eccentricities and slenderness ratios whereas supports were designed so as to eliminate rotation and twisting at the specimen ends. Kitipornchai and Lee [6] (1986) tested pin-ended equal-leg and unequal-leg single and double angles. 26 single equal and unequal angle struts, as well as 16 double equal and unequal angles were tested in this research. They concluded that the experimental results were in reasonable agreement with theoretical predictions calculated using design rules in AS 1250-1981 [7] and the AISC Specification [8]. Both specifications have adequate margins of safety for single and double angle struts. Al-Sayed and Bjorhovde [9] (1989) performed a study on 12 pin-ended steel angle columns. Adlari et al. [10] (1992) presented the behaviour of schifflerized hot-rolled angles (90° hot-rolled equal leg angles bent to 60°), typically used in mast structural systems. The overall buckling tests under concentric loading were performed. The sensitivity of these angles to torsion-flexural flexible buckling is emphasized, and design recommendations are given. A particular emphasis is placed on determining the applicable width for calculating the ratio of the width and thickness of the leg used in assessing the strength of the axially loaded compression members. In their paper, Adlari and Murty [11] (1996) presented the results obtained by experimental investigation of 26 hot-rolled steel angles. All specimens in this research were tested under concentric load with hinged end boundary conditions. Residual stresses and initial geometric imperfections were measured. Based on outcomes obtained in this investigation and the experimental results, the authors developed buckling curves for the prediction of ultimate buckling load [12]. Popovic et al. [13] (1999) tested a series of fixed-ended and pin-ended cold-formed steel plain angle columns. The authors noticed that the ultimate structural response of columns with slender angle sections is strongly affected by the eccentricity direction at column ends. The higher level of compressive stresses at the corner of the section, caused by load eccentricity applied towards the corner, reduces the stress level at the legs' tips and leads to higher compressive capacities in comparison with the corresponding columns where the eccentricity is applied toward the tips of the legs. Ben Young [14] (2004) conducted experimental tests on cold-formed steel plain angle columns compressed between fixed ends. The angle sections were brake-pressed from high strength structural steel sheets. The cold-formed lipped angles behaviour was investigated by Mohan et al. [15] (2006). The investigation included experimental tests of members as well as the testing of full-scale transmission tower panels, and subsequent comparison with the respective analytical and numerical calculations. Shifferaw et al. [16] (2006) tested cold-formed steel columns. The columns were 60 x 60 x 2.38 mm single and double angles. Young and Chen [17] (2008) performed an experimental investigation on cold-formed steel non-symmetric lipped angle columns. The experimental ultimate loads of the columns were compared with the design strengths calculated using the North American Specification [18] for the design of cold-formed steel structural members. It was shown that the design strengths are generally quite conservative for cold-formed steel non-symmetric lipped angle columns. Shi et al. [19] (2011) carried out an axial compression experiment on 420 MPa high strength steel equal angles, which included 15 stub columns. The test results were compared with the corresponding design methods in ANSI/AISC 360-05 [20] and Eurocode 3 [2]. The obtained design-strength values were higher than the ones given in ANSI/AISC 360-05 [20] and Eurocode 3 [2], and with the increase of width-to-thickness ratio, the differences between strength values became larger. Ke Cao et al. [21] (2015) performed a behavioural test of LHS columns (large-section and high-strength angle steel) under axial compression. The test included a total of 90 Q420 columns. The results of this study showed that the design codes GB 50017-2003 [22] and Eurocode 3 [2] are conservative. In their paper, Bhilawe and Gupta [23] (2015) reported results of compression tests on single equal angle sections connected to a gusset plate. The research included 12 single-bolt, 6 double-bolt and 6 welded-end fixity specimens. A. Landesmann et al. [24] (2017) reported the results of an experimental investigation on the behaviour and collapse of cold-formed steel short-to-intermediate pin-ended equal-leg angle columns with high slenderness values in the context of the development and performance assessment of a DSM-based design procedure.

Only a few studies have dealt with the compressive capacity of stainless steel angle columns. De Menezes et al. [25] (2019) presented experimental data for austenitic stainless steel angles subjected to compression. They tested hot-rolled equal-leg angles L 64 x 64 x 6.4 mm, with lengths varying from 250 mm to 1500 mm. The total of 13 samples were covered by this study. Experimental results were used to calibrate the developed numerical model whose parametric analysis consisted of 22 different cross-sections. The authors proposed new values of the imperfection factor α and limiting slenderness $\bar{\lambda}_0$, i.e. 0.60 and 0.23, respectively,

Table 1. Summary of database for angle column buckling tests

Reference	Steel material	Steel product	Cross-section dimensions mm]	No. of tests
[4]	Ugljični čelik	Hot-rolled angle	min. L32x32x3.2 - max. L152x19	170
[5]	SS 41	Hot-rolled angle	L90x90x7	57
[6]	Mild carbon steel f_y = 250 MPa	Hot-rolled angle	min. L64x64x5 - max. L102x76x6.5	42
[9]	Mild carbon-manganese steel f_y = 250 MPa	Hot-rolled angle	L76x76x10, L101x101x16, L127x127x10, L152x101x20	12
[10]	f_y = 333 - 475 MPa	Schifflerized hot-rolled angles	min. L76x76x6.4 - max. L102x102x6.4	18
[11]	f_y = 300 MPa	Hot-rolled angle	min. L64x64x9.5 - max. L127x9.5	26
[13]	f_y = 350 MPa	Cold-formed angle	L50x50x2.5, L50x50x4, L50x50x5	30
[14]	G500 i G450	Cold-formed angle	L70x70x1.2, L70x70x1.5, L70x70x1.9	24
[15]	f_y = 350 MPa	Cold-formed lipped angle	L75x75x30x3.15	11
[16]	f_y = 375 MPa	Cold-formed angle	L60x60x2.38	12
[17]	G550 i G450	Cold-formed lipped angle	L80x50x16x1 L80x50x16x1.5 L80x50x16x1.9	25
[19]	Q420	Hot-rolled angle	min. L125x125x8 - max. L200x200x14	15
[21]	Q420	Hot-rolled angle	min. L220x220x20 - max. L250x250x30	90
[23]	Mild steel f_y = 350 MPa	Hot-rolled angle	L50x50x6, L60x60x5, L65x65x6	24
[24]	ZAR-345 mild steel	Cold-formed angle	min. L50x50x1.55 - max. L90x90x1.55	20
[25]	Austenitic stainless steel	Hot-rolled angle	L64x64x6.4	13

for columns with stocky hot-rolled equal angle sections made of austenitic stainless steel.

A summary of the database for buckling tests of angle columns is given in Table 1.

2. Experimental testing of material

The experimental investigation was concentrated on the austenitic stainless steel grade EN 1.4301 (X5CrNi18-10). This is the most widely used grade of stainless steel used in structural applications.

Tensile testing of coupons was performed in the Metals laboratory at the University of Belgrade Faculty of Technology and Metallurgy. The tests were carried out on a Shimadzu Universal Testing Machine AG-Xplus. The coupons were tested in accordance with EN ISO 6892-1 [26]. Three flat coupons were longitudinally cut from both legs of the hot-rolled specimen (see Figure 2).

Figure 2. Location of coupons from hot-rolled angle specimens

All coupons were cut by a water jet cutter to decrease heating of material during preparation. The coupons were 12.5 mm wide in the necked region. A calibrated extensometer with a gauge length of L_0 = 50 mm was used for longitudinal strain measurement. The adopted strain rates were 0.1 mm/min for the initial part of the test up to approximately 1 % total strain after which it was increased to 2.0 mm/min. A typical coupon prior to and after testing is shown in Figure 3.

Figure 3. Tensile test setup and stainless steel coupon before and after testing

The engineering stress–strain curves obtained for all three tensile coupons are provided in Figure 4. Material properties including the yield strength f_y used as the 0.2

Table 2. Material properties from tensile coupon tests and according to Specifications [1, 27]

Coupons from hot-rolled angle section EN 1.4301	$f_{0.2}$ [N/mm²]	$\sigma_{0.01}$ [N/mm²]	$\sigma_{0.05}$ [N/mm²]	$\sigma_{1.0}$ [N/mm²]	f_u [N/mm²]	E [N/mm²]	ε_u [%]	ε_f [%]	Strain hardening parameters	
									n	*m*
Coupon 1	281	200	244	350	655	199604	52	71	8	2.8
Coupon 2	288	201	242	375	661	197161	51	65	8	3.5
Coupon 3	294	203	248	363	658	199924	53	67	8	2.9
Average	288	201	244	363	658	198896	52	67	8	3.1
EN 10088-5 & EN 1993-1-4	190	-	-	225	500-700	200000	-	45	6	-

% proof stress $f_{0.2}$, the ultimate tensile strength f_u, various proof stresses ($\sigma_{0.01}$, $\sigma_{0.05}$ and $\sigma_{1.0}$), the strain corresponding to the ultimate tensile strength ε_u, total strain at fracture ε_f, and the modulus of elasticity E, including the strain hardening parameters n and m, were recorded and reported in Table 2. Additionally, Table 2 presents a comparison of their average values with equivalent nominal values given in EN 10088-5 [27] and EN 1993-1-4 [1], respectively. In mathematical interpretation of nonlinear behaviour of stainless steel, the strain hardening parameters n and m depict the degree of nonlinearity of the stress–strain curve through two different stages presented by two modified Ramberg–Osgood equations [28]. The experimental strain hardening parameters n and m (see Table 2) were obtained using a computer programme based on the least squares regression method [29] so that every experimental stress–strain curve closely matches the predictive curves developed by the Ramberg–Osgood equations [28], minimizing the error between them.

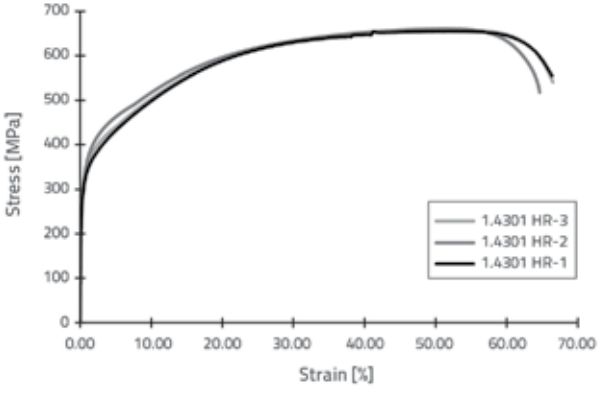

Figure 4. Engineering stress-strain curves

It can be seen from Table 2 that the average measured yield strength exceeds the nominal value by a margin of 52 %. According to EN 10088-5 [27], the yield strength f_y and ultimate tensile strength f_u refer to the minimum specified values for the 0.2 % proof strength $R_{p0.2}$ and tensile strength R_m that are obtained for stainless steel materials in the annealed conditions. Annealing is a heat treatment process employed to ensure an optimized corrosion resistance, softness and ductility of the material, and to reduce residual effects from manufacturing processes such as welding or bending. However, austenitic stainless steels cannot be hardened by heat treatment. The yield strength $f_{0.2}$ = 190 MPa is relatively low (see Table 2) in the annealed state. On the other hand, strength levels of austenitic stainless steels can by significantly increased by cold working during the fabrication process considering their high strain hardening parameters. Thus, the specified nominal values [1, 27] are conservative for the profiles that undergo further finishing processes after hot-rolling, such as straightening, cold drawing or sectional machining.

3. Resistance of compressed angle members according to Eurocode 3

The design method for calculating the buckling resistance of compressed angle columns, which is given in EN 1993-1-1 [2] and EN 1993-1-3 [3], is based on the theoretical solution of elastic stability of compressed thin-walled monosymmetric and asymmetric section members [30]. In the case of pin-ended columns, the lowest elastic buckling load N_{cr} is the lowest solution of the following equation:

$$\begin{aligned}&\left(N_{cr,u}-N_{cr}\right)\left(N_{cr,v}-N_{cr}\right)\left(N_{cr,T}-N_{cr}\right)i_0^2\\&-N_{cr}^2\left[\left(N_{cr,u}-N_{cr}\right)v_0^2+\left(N_{cr,v}-N_{cr}\right)u_0^2\right]=0\end{aligned} \quad (1)$$

where $N_{cr,u}$ and $N_{cr,v}$ are the elastic critical forces for flexural buckling about the major u-u and minor v-v principal axes, respectively, while $N_{cr,T}$ is the elastic critical force for torsional buckling:

$$N_{cr,u}=\frac{\pi^2 EI_u}{L^2} \quad (2)$$

$$N_{cr,v}=\frac{\pi^2 EI_v}{L^2} \quad (3)$$

$$N_{cr,T}=\frac{1}{i_0^2}\left(GI_t+\pi^2\frac{EI_w}{L^2}\right) \quad (4)$$

In the above equations, I_u and I_v are the second moments of inertia about the major and minor principal cross-section axes, I_t is the torsional constant, I_w is the warping constant, L is the buckling length, E is the modulus of elasticity, and G is the shear modulus.
The i_0^2 in Eq. (1) is determined as follows:

$$i_0^2 = i_v^2 + i_u^2 + v_0^2 + u_0^2 \quad (5)$$

where i_u and i_v are the radii of gyration about the major and minor principal axes, respectively, and v_0 and u_0 are the coordinates of the shear centre relative to the centroid of the cross-section.
For equal-leg angle columns, $v_0 = 0$ and Eq. (1) is simplified as

$$(i_0^2 - u_0^2)N_{cr}^2 - i_0^2(N_{cr,u} + N_{cr,T})N_{cr} + i_0^2 N_{cr,u} N_{cr,T} = 0 \quad (6)$$

gdje je:

$$N_{cr} = \min\left(N_{cr,v}; N_{cr,TF}\right) \quad (7)$$

where $N_{cr,TF}$ represents the elastic critical flexural-buckling force:

$$N_{cr,TF} = \frac{N_{cr,u}}{2\left(1-\frac{u_0^2}{i_0^2}\right)}\left[1+\frac{N_{cr,T}}{N_{cr,u}} - \sqrt{\left(1+\frac{N_{cr,T}}{N_{cr,u}}\right)^2 - 4\left(1-\frac{u_0^2}{i_0^2}\right)\frac{N_{cr,T}}{N_{cr,u}}}\right] \quad (8)$$

Once the elastic critical force N_{cr} has been determined, the compression resistance $N_{b,Rd}$ is found from the well-known Perry-Robertson equation by using a linear expression between the imperfection factor and the member non-dimensional slenderness [2].

4. Finite element analysis

A Finite Element Analysis (FEA), presented in this section, focuses on pin-ended stainless steel equal-leg angle columns with nominal cross-section dimensions 60 x 6 mm (leg width x thickness). To assess the appropriateness of buckling curve *b* used for the design of hot-rolled carbon steel equal-leg angle columns [2] for the design of equivalent stainless steel angle columns, and to provide a smooth elastic-to-inelastic buckling transition, the lengths of FE models were selected to cover a wide range of overall geometric slenderness values. The analysed range of overall slenderness ratios about the minor principal axis of the angle section is 15–256. Additionally, parametric sensitivity studies were performed to investigate the influences of initial imperfections, material nonlinearities, and residual stresses on compressive capacities of stainless steel hot-rolled angle columns. A geometrically and materially nonlinear analysis was performed using the ABAQUS FE software package [31], employing its explicit dynamic solver since it has already been successfully used for simulation of column buckling tests [32].

4.1. Geometry, boundary conditions and mesh

Hot-rolled angle columns are modelled with their nominal geometry. Eight node hexahedron solid elements with reduced integration (C3D8R) are used for the angle legs, while six-node wedge elements (C3D6) are used for corner regions, since they offer good results for a reasonable computation time. A global element size of 2 mm is used for each FE model with at least three elements through legs' thickness in order to properly take into account their bending stiffness. Support and loading zones on the column ends are kinematically constrained to reference points in order to model the hinge-supported behaviour of the columns. The reference points are set at the centroids of columns' end cross-sections. Failure loading is applied as displacement-controlled to a reference point in the loading zone. The geometry, mesh and boundary conditions of the FE model representing the column buckling test are shown in Figure 5.

Figure 5. FE model geometry and boundary conditions

4.2. Material modelling

To account for the nonlinear material law, the mechanical properties obtained from the first tensile coupon test (see Table 2) are assigned to each FE model. Plasticity with isotropic hardening is used with an initial modulus of elasticity E = 200 GPa, and Poisson's ratio ν = 0.3.
An engineering stress–strain curve is transformed to a true stress–strain curve for input in the ABAQUS plasticity model, using Equations (9) and (10), where σ_{nom} and ε_{nom} are the engineering stress and strain, E is the modulus of elasticity, σ_{true} and ε_{ln}^{pl} are the true stress and logarithmic plastic strain, respectively. Figure 6 shows the engineering stress–strain curve obtained from the first tensile coupon test and the corresponding true stress–strain curve that is introduced in FE models.

$$\sigma_{true} = \sigma_{nom}(1+\varepsilon_{nom}) \quad (9)$$

$$\varepsilon_{ln}^{pl} = \ln(1+\varepsilon_{nom}) - \sigma_{true}/E \quad (10)$$

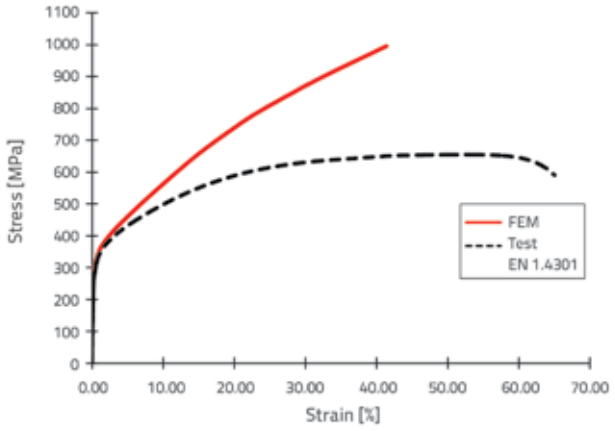

Figure 6. Engineering and true stress–strain curves

4.3. Geometric imperfections

The superposition of initial geometric imperfections in the shape of the lowest overall flexural buckling mode with an amplitude of $\delta_0 = L/1000$ (0.1 % of the column length L) and the lowest torsional-flexural buckling mode with an amplitude of $\varphi_0 = t/10$ (10 % of the leg thickness t) is assigned to all FE models. This approach is based on papers by Landesmann et al. [33] and Dinis and Camotim [34] that showed that the adopted distributions and amplitude values of initial geometric imperfections may sufficiently capture the behaviour of carbon steel angle columns with reasonable accuracy relative to experimental results. The amplitude value of $L/1000$ of the initial out-of-straightness corresponds to 75 % of the maximum permitted imperfections for essential tolerances according to EN 1090-2 [35], as stated in Annex C of EN 1993-1-5 [36]. However, it should be noted that the European Standard that specifies tolerances on shape dimensions and mass of hot-rolled structural steel angles, EN 10056-2 [37], limits the straightness tolerances to $0.4\ \%\cdot L$ for leg length of less than or equal to 150 mm. Hence, for the considered angle section measuring 60 x 6 mm, the adopted amplitude of the initial out-of-straightness corresponds to 25 % of the maximum permitted tolerance in accordance with EN 10056-2 [37]. Each buckling mode shape is determined by means of a preliminary eigenvalue Linear Buckling Analysis (LBA), performed with the same mesh and employed to carry out the subsequent nonlinear buckling analysis. The eigenmodes obtained by LBA are shown in Figure 7. Considering that the sign of the initial out-of-straightness is not explicitly defined in Specifications [35, 37], and that it is not obvious without previous measurements, both directions of imperfection distributions were employed in the nonlinear buckling analysis: in the positive directions related to deformed buckling shapes of FE models obtained in the LBA, and in negative directions that are opposite to the directions of the deformed buckling shapes of FE models in the LBA.

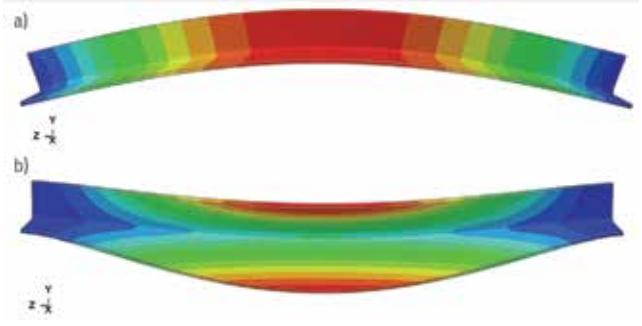

Figure 7. Eigenmodes obtained by LBA

4.4. Residual stresses

The magnitude and distribution of residual stresses in structural sections is significantly dependent on the production process. The level of residual stresses in hot-rolled stainless steel sections depends on the annealing temperature, cooling conditions, level of cold working, cross-section geometry, and stainless steel grade. Distinctions between the material and thermal properties of carbon steel

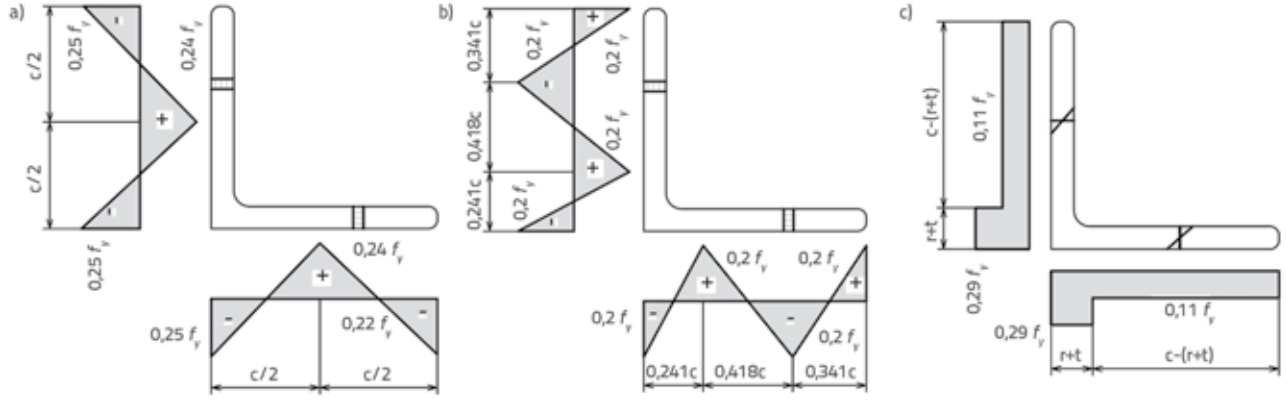

Figure 8. Residual stress distribution models of hot-rolled equal-leg angles a) Three-point RS predictive model with uniform distribution [38]; b) Four-point RS predictive model with uniform distribution [39]; c) Bending RS predictive model with linear distribution [41]

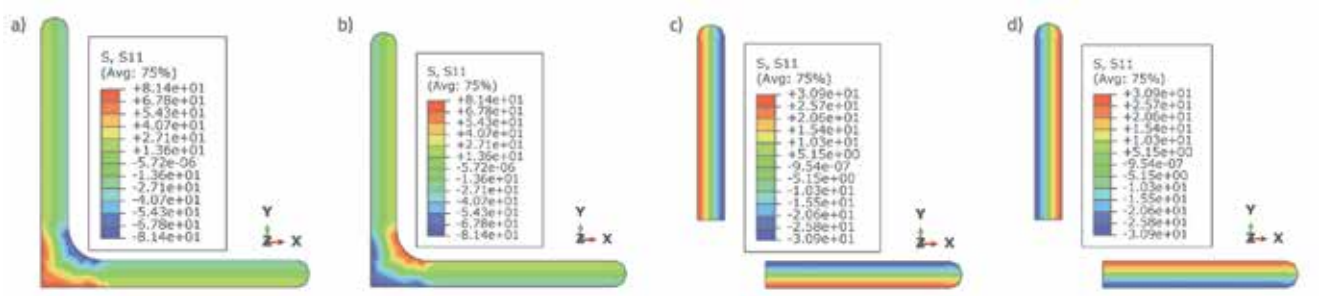

Figure 9. Residual stresses applied to FE model: a) Distribution of RS⁺ through section thickness; b) Distribution of RS⁺ through leg thickness; c) Distribution of RS⁻ through section thickness; d) Distribution of RS⁻ through leg thickness

and stainless steel cause differences in the magnitude and distribution of residual stresses in structural sections of these two materials. The coefficient of thermal expansion of austenitic stainless steel is higher than that of structural carbon steel, while the thermal conductivity is lower, which consequently leads to larger residual stresses relative to carbon steel. Numerous research into the effect of residual stresses has been carried out for carbon steel angles.

A linear three-point predictive model of the distribution of residual stresses in hot-rolled carbon steel equal-leg angle sections, presented in Figure 8a, was used for developing ECCS buckling curves [38]. The distribution is symmetrical with compressive stresses at the legs' intersection and at their ends, and equilibrating tensile stresses at the legs' mid-length. In parallel, Figure 8b shows a linear four-point predictive model that was based on comprehensive measurements of residual stresses in large carbon steel equal-leg angles [39]. In both predictive models, it is assumed that the distribution of residual stresses is uniform throughout the thickness of the section with the dominant membrane stress component. While the patterns of residual stresses in structural carbon steel sections have been extensively studied, the data on residual stresses in hot-rolled stainless steel structural shapes are limited. Cruise and Gardner [40, 41] carried out an extensive experimental program to quantify the distribution of residual stresses in hot-rolled and cold-formed stainless steel sections including hot-rolled equal-leg angle specimens with nominal dimensions 50 x 3 mm. All sections were manufactured using the austenitic stainless steel grade EN 1.4301. Cruise and Gardner's research approach [40, 41] takes into account the total residual stress that includes both membrane and bending component. The membrane component corresponds to compressive or tensile axial deformation, while the bending component linearly varies through the thickness of the section. However, the authors found that both bending and membrane residual stress components are relatively low in the case of hot-rolled stainless steel angles. Based on experimental results, they proposed a simple predictive model for bending residual stresses assuming their linear variation through thickness with either tensile or compressive values at the outer surface of the angle-section. The proposed model based on mean values of the measured stresses [41] is shown in Figure 8c. This predictive model is indirectly applied in each FE model by equivalent temperature strains as an initial state of the non-linear buckling analysis to represent an equilibrium stress state in the first load step of the calculation. The formulation of predefined analytical fields is employed to assign the desired stress values and different signs through legs thickness. The bending residual stress values of $0.29 \cdot f_y$ = 81.5 MPa and $0.11 \cdot f_y$ = 30.9 MPa were set in the corner and flat regions, respectively. Two opposite patterns are considered, positive distribution with compressive stresses at the outer section surface (RI⁺), and negative distribution with tensile stresses at the outer section surface (RI⁻). It can be seen in Figure 9 that a very good application of residual stresses to FE model has been achieved.

5. Discussion of results

5.1. FE sensitivity study

In this section, the compressive capacities of stainless steel angle columns obtained in the FE sensitivity study are compared with compressive capacities of the equivalent initially straight columns without residual stresses (see Table 3). As previously mentioned, the FE sensitivity study considers separate and combined effects of initial geometric imperfections and residual stresses on ultimate buckling responses of stainless steel angle columns. Table 4 quantifies the decrease of column buckling resistance of initially perfect columns caused by influences of separate and combined actions of geometric imperfections (GI) and residual stresses (RS) accounting for the change of sign of their distributions.

A brief analysis of the obtained results is presented as follows. The ultimate structural response of FE models involves local buckling of angle legs, torsional–flexural mode under combined twisting and major axis flexural deflection, and flexural buckling mode about the minor principal axis.

Individual actions of residual stresses slightly influence compressive capacities of stainless steel angle columns in the low and intermediate slenderness range, up to λ_v = 60. However, these effects are more significant in the high

Table 3. FE ultimate buckling loads considering effects of initial GI and RS

FE models	FE ultimate buckling loads $N_{b.u.FEA}$ [kN]								
Length [mm]	without GI & RS	Individual effects of GI and RS				Combined effects of GI and RS			
		without GI & with RS^+	without GI & with RS^-	without RS & with GI^+	without RS & with GI^-	with GI^+ & RS^+	with GI^+ & RS^-	with GI^- & RS^+	with GI^- & RS^-
	$N_{b.u.FEA.1}$	$N_{b.u.FEA.2}$	$N_{b.u.FEA.3}$	$N_{b.u.FEA.4}$	$N_{b.u.FEA.5}$	$N_{b.u.FEA.6}$	$N_{b.u.FEA.7}$	$N_{b.u.FEA.8}$	$N_{b.u.FEA.9}$
180	231.8	231.1	232.5	207.2	207.2	207.4	207.4	207.1	207.1
250	210.8	210.5	211.1	201.4	201.4	201.4	201.4	201.4	201.4
300	198.7	198.7	198.7	199.5	190.4	199.6	199.5	190.4	190.5
400	181.2	180.9	181.5	176.9	171.9	177.1	176.8	171.6	172.3
500	167.4	168.2	166.5	160.6	157.2	160.6	161.0	158.1	156.9
600	157.0	155.7	159.1	147.6	144.8	147.6	147.5	144.4	145.2
650	151.3	151.2	154.9	141.9	138.8	142.1	140.8	137.5	137.5
700	148.2	147.0	155.6	135.6	132.8	136.3	134.9	131.4	134.2
800	146.2	142.8	149.3	125.5	122.5	124.3	127.0	124.6	121.0
1000	139.5	131.9	141.6	105.7	103.2	108.9	104.1	101.7	105.6
1200	117.3	105.9	115.6	85.5	84.0	87.5	83.0	81.1	86.8
1400	103.8	87.6	92.8	68.4	66.8	71.6	66.7	65.9	70.3
1600	95.5	76.9	81.4	56.8	55.5	60.2	55.2	54.8	59.6
1800	89.2	66.0	70.2	47.5	46.4	51.6	45.2	44.3	50.4
2000	84.3	64.8	68.2	40.4	39.4	43.2	38.2	37.6	41.5
2200	79.9	54.6	57.8	34.8	34.0	39.0	32.9	32.3	37.8
2400	77.1	48.7	50.8	30.7	30.0	36.8	26.3	25.4	36.3
2800	74.1	45.9	48.7	25.3	24.6	28.0	22.5	22.3	27.7
3000	72.5	42.5	46.1	23.5	22.9	26.6	21.5	21.3	25.7

Table 4. Quantification of initial GI and RS influences on FE ultimate buckling loads

FE modeli		Ratios of FEA ultimate buckling loads							
Length [mm]	Slenderness ratio λ_v	Individual effects of GI and RS				Combined effects of GI and RS			
		$N_{b.u.FEA.2}$ / $N_{b.u.FEA.1}$	$N_{b.u.FEA.3}$ / $N_{b.u.FEA.1}$	$N_{b.u.FEA.4}$ / $N_{b.u.FEA.1}$	$N_{b.u.FEA.5}$ / $N_{b.u.FEA.1}$	$N_{b.u.FEA.6}$ / $N_{b.u.FEA.1}$	$N_{b.u.FEA.7}$ / $N_{b.u.FEA.1}$	$N_{b.u.FEA.8}$ / $N_{b.u.FEA.1}$	$N_{b.u.FEA.9}$ / $N_{b.u.FEA.1}$
180	15	1.00	1.00	0.89	0.89	0.89	0.89	0.89	0.89
250	21	1.00	1.00	0.96	0.96	0.96	0.96	0.96	0.96
300	26	1.00	1.00	0.99	0.96	1.00	1.00	0.96	0.96
400	34	1.00	1.00	0.98	0.95	0.98	0.98	0.95	0.95
500	43	1.00	0.99	0.96	0.94	0.96	0.96	0.94	0.94
600	51	0.99	1.01	0.94	0.92	0.94	0.94	0.92	0.93
650	55	1.00	1.02	0.94	0.92	0.94	0.93	0.91	0.91
700	60	0.99	1.05	0.92	0.90	0.92	0.91	0.89	0.91
800	68	0.98	1.02	0.86	0.84	0.85	0.87	0.85	0.83
1000	85	0.95	1.02	0.76	0.74	0.78	0.75	0.73	0.76
1200	102	0.90	0.98	0.73	0.72	0.75	0.71	0.69	0.74
1400	119	0.84	0.89	0.66	0.64	0.69	0.64	0.64	0.68
1600	136	0.81	0.85	0.59	0.58	0.63	0.58	0.57	0.62
1800	153	0.74	0.79	0.53	0.52	0.58	0.51	0.50	0.56
2000	170	0.77	0.81	0.48	0.47	0.51	0.45	0.45	0.49
2200	187	0.68	0.72	0.44	0.43	0.49	0.41	0.40	0.47
2400	204	0.63	0.66	0.40	0.39	0.48	0.34	0.33	0.47
2800	239	0.62	0.66	0.34	0.33	0.38	0.30	0.30	0.37
3000	256	0.59	0.64	0.32	0.32	0.37	0.30	0.29	0.35

slenderness range. The maximum decrease of ultimate buckling resistance of initially perfect stainless steel angle columns (λ_v = 256) influenced by separate action of residual stresses is 41 %. The positive distribution of residual stresses (RI^+) causes a lower column buckling resistance compared to their negative distribution (RI^-), with differences of up to 8 % (see Table 3).

As expected, initial geometric imperfections affect the column buckling resistance more adversely compared to residual stresses. The sine wave shape of initial geometric imperfections with an amplitude of *L*/1000 at column mid-height and with leg ends on the concave side (GI^-) reduces the ultimate strength of a perfectly straight column from 4 % in the low slenderness range (λ_v = 21–26), to up to 68 % in the high slenderness range (λ_v = 256). Even though the symmetric shape of geometric imperfections with a positive sign (GI+) causes a slightly smaller reduction of compressive capacity of an initially perfect angle column relative to the GI^- distribution, these differences of up to 2 % are considered negligible.

The combined effects of the residual stresses and initial out-of-straightness do not reach the sum of their individual effects on the buckling resistance of stainless steel angle columns in the entire analysed slenderness range. However, it can be seen from Table 4 that these detrimental effects are not significantly higher than those caused by individual action of initial geometric imperfections. The study indicates that interaction effects of residual stresses (RS^+) and geometric imperfections (GI^-) leads to the lowest values of ultimate buckling loads. It should be noted that for this case, the deformed shape of stainless steel angle columns at the ultimate limit state is the same as the deformed shape caused by individual action of both GI^- and RS^+.

5.2. Comparison of FE buckling resistance with design buckling resistance

Minimum values of FE ultimate buckling loads (see Table 3) are used to assess the appropriateness of the predictive method for the design of centrically compressed angle members according to Eurocodes EN 1993-1-4 [1] and EN 1993-1-1 [2]. Material properties obtained from the first tensile coupon test (see Table 2), limiting slenderness $\bar{\lambda}_0$ = 0.2, and partial safety factor γ_{M1} = 1.0 are employed in the calculation of the column buckling resistance $N_{b,u,EC}$. Depending on the overall slenderness, the predicted failures of stainless steel angle columns occur due to torsional-flexural buckling or flexural buckling about the minor principal axis.

Graphical comparison between the Eurocode buckling curves and the normalised FE buckling loads is presented in Figure 10. The FE ultimate loads are normalised by dividing by the squash load Af_y and are plotted against the column non-dimensional slenderness. Figure 10 shows that most of the FE results lay between curves *c* and *b* and, hence, these curves have been selected for evaluation as representative for predicting flexural buckling modes of stainless steel equal-angle columns. Additionally, in order to evaluate accuracy of the design method for torsional-flexural buckling mode, the buckling curve *b* is used as stated in EN 1993-1-4 [1].

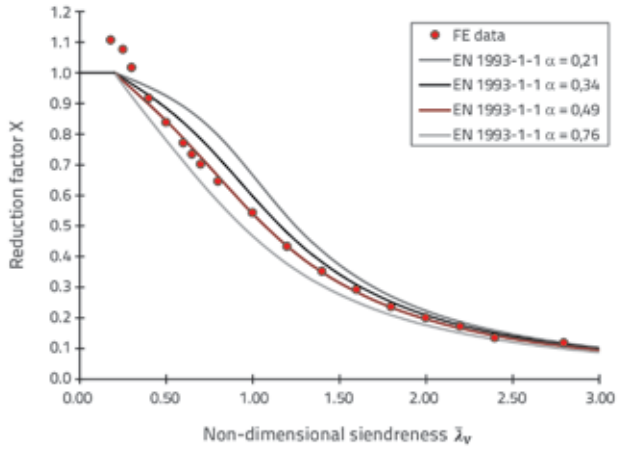

Figure 10. Comparison between normalised FE results and Eurocode 3 buckling curves

It should be emphasized that the change of buckling curve for calculation of ultimate loads for flexural buckling modes also affects prediction of the torsional-flexural failure mode. The comparison of FE results and selected curves is presented in Figure 11. If curve *b* is selected for the flexural buckling mode, the mean FE-to-predicted buckling load ratio $N_{Fb,u,FE}/N_{Fb,u,EC}$ is 0.95 and the Coefficient of Variation (CoV) is 7.6 %, while in the case of the torsional-flexural mode, the mean FE-to-predicted buckling load ratio $N_{TFb,u,FE}/N_{TFb,u,EC}$ is 1.12 and the CoV is 15 %. However, curve *c* follows closely the trend of the FE points and more safely represents the flexural behaviour of stainless steel equal-angle columns: the mean ratio $N_{Fb,u,FE}/N_{Fb,u,EC}$ is 1.02, and the CoV is 6.0 %. Consequently, a smaller scatter of data for the torsional-flexural mode is obtained, the mean ratio $N_{TFb,u,FE}/N_{TFb,u,EC}$ is 1.2, and the CoV is 10.5 %.

6. Conclusions

An FE study of austenitic stainless steel hot-rolled equal-angle columns was performed based on an experimental non-linear material model and a predictive residual stress model [41].

The FE sensitivity study was conducted to quantify the level of individual and combined effects of initial geometric imperfections and residual stresses considering their different distribution signs. It was established that the combination of initial geometric imperfections in the direction opposite to the lowest buckling shape obtained in the LBA, and a residual stress pattern with tensile stresses at the outer surface of the angle section, leads to the lowest value of ultimate buckling load of stainless steel equal angle columns. However, the combined

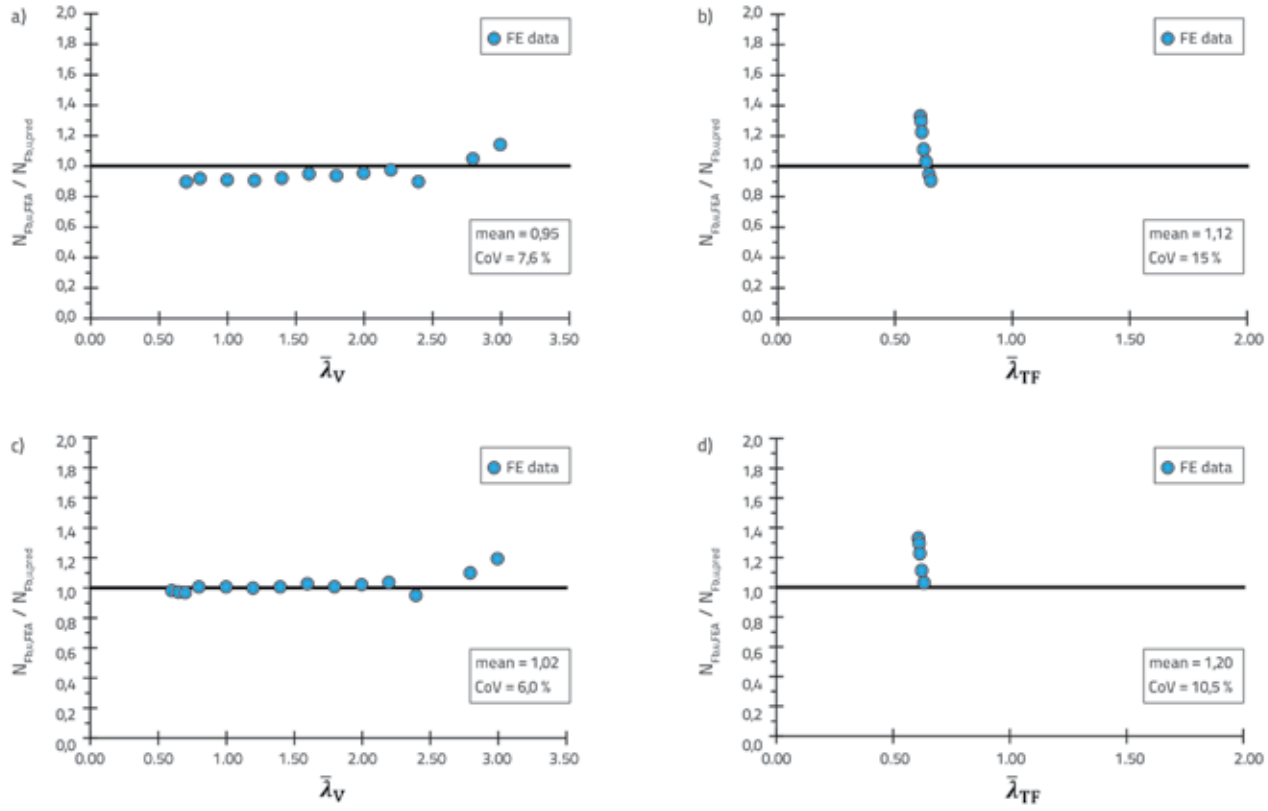

Figure 11. Comparison of design predictions and FE results, Comparison between FE and DESIGN: a) flexural buckling loads when curve b is selected for the flexural buckling mode; b) torsional-flexural buckling loads when curve b is selected for the flexural buckling mode; c) flexural buckling loads when curve c is selected for the flexural buckling mode; d) torsional-flexural buckling loads when curve c is selected for the flexural buckling mode

weakening effects due to geometric imperfections and residual stresses are not considerably higher when compared to individual influences of geometric imperfections

The FE results were used to assess the accuracy of existing Eurocode provisions for column design [1, 2], including the appropriateness of buckling curves *b* and *c*. The study indicated that the buckling curve *c* represents more consistently and safely the non-linear behaviour and ultimate capacity predictions of stainless steel hot-rolled equal-angle columns in comparison with curve *b* that is employed for the design of equivalent carbon steel columns. Considering curve *c*, the mean ratio of $N_{b,u,FE}/N_{Fb,u,EC}$ is 1.02 and the CoV is 6.0 %, while for buckling curve *b*, the mean value of the $N_{b,u,FE}/N_{Fb,u,EC}$ ratio is 0.95 and the CoV is 7.6 %.

The database developed in this study is limited to the definition of explicit design provisions. This points to the need for carrying out an experimental programme supported by theoretical and numerical analyses so as to find more accurate and reliable solutions on this issue.

Acknowledgements

This investigation is supported by the Serbian Ministry of Education, Science and Technological Development through the TR-36048 project. The authors are grateful to companies *Montanstahl ag Switzerland, Vetroelektrane Balkana Belgrade, Armont SP Belgrade, Institute for Testing of Materials Belgrade, Institute for Materials and Structures Faculty of Civil Engineering University of Belgrade, ConPro Novi Sad, Energoprojekt Industrija PLC Belgrade, Vekom Geo Belgrade, CO-Designing, Peri Oplate Belgrade, North Engineering Subotica, Amiga Kraljevo, Mašinoprojekt kopring PLC Belgrade, Sika Belgrade, DvaD Solutions Belgrade and Soko Inžinjering Belgrade, for their extensive support.*

REFERENCES

[1] Eurocode 3: Design of steel structures - part 1-4: General rules - supplementary rules for stainless steels, including amendment A1 (2015), EN 1993-1-4:2006+A1:2015, Brussels, Belgium, CEN 2015.

[2] Eurocode 3: Design of steel structures - Part 1-1: General rules and rules for buildings EN 1993-1-1, Brussels, Belgium, CEN 2005.

[3] Eurocode 3: Design of Steel Structures - Part 1-3: General rules - Supplementary rules for cold-formed members and sheeting EN 1993-1-3, Brussels, Belgium, 2006.

[4] Stang, A.H., Strlckenberg, L.R.: Results of some compression test of structural steel angles, U.S. Bureau of Standards, Technologic Papers No. 218, Govt. Printing Ofc., Washington, D.C. 1924

[5] Wakabayashi, M., Nonaka, T.: On the buckling strength of angles in transmission towers, Bull., Disaster Prevention Res. Inst., Kyoto Univ., Japan, 15 (1965) 91, pp. 1-18.

[6] Kitipornchai, S., Lee, H.W.: Inelastic experiments on angle and tee struts, J. Constr. Steel Res., London, England, 6 (1986) 3, pp. 219-236, https://doi.org/10.1016/0143-974X(86)90035-0

[7] AS 1250-1981 SAA Steel Structures Code, Standards Association of Australia, Sydney, Australia, 1981.

[8] Specification for the Design, Fabrication and Erection of Standard Steel for Buildings, American Institute of Steel Construction, New York. NY, 1978.

[9] Al-Sayed, S.H., Bjorhovde, R.: Experimental study of single angle columns, J. Constr. Steel Res., London, England, 12 (1989) 2, pp. 83-102, https://doi.org/10.1016/0143-974X(89)90026-6

[10] Adluri, S.M.R.A, Madugula, M.K.S., Monforton G.R.: Schifflerized angle struts, J. Struct. Eng., 118 (1992) 7, pp. 1920-1936, https://doi.org/10.1061/(ASCE)0733-9445(1992)118:7(1920)

[11] Adluri, S.M.R.A., Madugula, M.K.S.: Flexural buckling of steel angles: experimental investigation, J. Struct. Eng., 122 (1996) 3, pp. 309-317, https://doi.org/10.1061/(ASCE)0733-9445(1996)122:3(309)

[12] Adluri, S.M.R.A., Madugula, M.K.S.: Development of column curve for steel angles, J. Struct. Eng., 122 (1996) 3, pp. 318-325, https://doi.org/10.1061/(ASCE)0733-9445(1996)122:3(318)

[13] Popovic, D., Hancock, G.J., Rasmussen, K. J. R.: Axial compression tests of cold-formed angles, J. Struct. Eng., 125 (1999) 5, pp. 515-523, https://doi.org/10.1061/(ASCE)0733-9445(1999)125:5(515)

[14] Young, B.:Tests and Design of Fixed-Ended Cold-Formed Steel Plain Angle Columns, J. Struct. Eng., 130 (2004) 12, pp. 1931-1940, https://doi.org/10.1061/(ASCE)0733-9445(2004)130:12(1931)

[15] Mohan, S.J., Rahima Shabeen, S., Samuel Knight, G.M.: Behaviour of cold formed lipped angles in transmission line towers, Thin-Walled Structures, 44 (2006), pp. 1017-1030, https://doi.org/10.1016/j.tws.2006.07.006

[16] Shifferaw Y., Malite, M., Schafer B.W., Chodraui, G.M.B.: Cold-formed Steel Angles under Axial Compression - 18th International Specialty Conference on Cold-Formed Steel Structures, 2006.

[17] Young, B., Chen J.: Column tests of cold-formed steel non-symmetric lipped angle sections", Journal of Constructional Steel Research, 64 (2008), pp. 808-815, https://doi.org/10.1016/j.jcsr.2008.01.021

[18] NAS. North American Specfication for the design of cold-formed steel structural members. North American Cold-formed Steel Specfication. Washington (DC): American Iron and Steel Institute; 2001.

[19] Shi, G., Liu, Z., Ban, H.Y., Zhang, Y., Shi, Y.J., Wang, Y.Q.: Tests and finite element analysis on the local buckling of 420 MPa steel equal angle columns under axial compression, Steel and Composite Structures, 12 (2011) 1, pp. 31-51, https://doi.org/10.12989/scs.2012.12.1.031

[20] ANSI/AISC 360-16, Specification for Structural Steel Buildings, American Institute of Steel Construction, Chicago, 2016.

[21] Cao, K., Guo, Y., Zeng, D.: Buckling behavior of large-section and 420 MPa high-strength angle steel columns, Journal of Constructional Steel Research, 111 (2015), pp. 11-20

[22] GB50017-2003. Code for design of steel structures. Beijing: China Architecture & Building Press; 2003

[23] Bhilawe, J.V., Gupta, L.M.: Experimental investigation of steel equal angle subjected to compression, Engineering Structures and Technologies, 7 (2015) 2, pp. 55-66, https://doi.org/10.3846/2029882X.2015.1113892

[24] Landesmann, A., Camotim, D., Dinis, P.B., Cruz, R.: Short-to-intermediate slender pin-ended cold-formed steel equal-leg angle columns: Experimental investigation, numerical simulations and DSM design, Engineering Structures, 132 (2017), pp. 471-493, https://doi.org/10.1016/j.engstruct.2016.11.034

[25] de Menezes, A.A., da S. Vellasco, P.C.G., de Lima, L.R.O., da Silva, A.E.: Experimental and numerical investigation of austenitic stainless steel hot-rolled angles under compression, Journal of Constructional Steel Research, 152 (2019), pp. 42-56, https://doi.org/10.1016/j.jcsr.2018.05.033

[26] EN ISO 6892-1, Metallic materials — tensile testing, Part 1: Method of Test at Room Temperature. European Committee for Standardization, CEN, Brussels, 2009.

[27] EN 10088: Stainless steels - Part 5: Technical delivery conditions for bars, rods, wire, sections and bright products of corrosion resisting steels for construction purposes, European Standard CEN, 2009.

[28] Arrayago, I., Real, E., Gardner, L.: Description of stress-strain curves for stainless steel alloys, Mater. Des., 87 (2015), pp. 540-552.

[29] Dobrić, J., Budjevac, D., Marković, Z., Gluhović, N.: Behaviour of stainless steel press-braked channel sections under compression, J. Constr. Steel Res., 139 (2017), pp. 236-253, https://doi.org/10.1016/j.jcsr.2017.09.005

[30] Timoshenko, S., Gere, J.M.: Theory of elastic stability, Engineering Societies Monograph, McGraw-Hill, New York, 1961.

[31] ABAQUS User Manual, Version 6.12, Providence RI, USA: DS SIMULIA Corp, 2012.

[32] Dobrić, J., Pavlović, M., Marković, Z., Buđevac, D., Spremić, M.: Resistance of cold-formed built-up stainless steel members - Part II: Numerical simulation, J. Construct. Steel Res., 140 (2018), pp. 247-260.

[33] Landesmann, A., Camotim, D., Dinis, P.B., Cruz, R.: Short-to-intermediate slender pin-ended cold-formed steel equal-leg angle columns: Experimental investigation, numerical simulations and DSM design, Engineering Structures, 132 (2017), pp. 471-493, https://doi.org/10.1016/j.engstruct.2016.11.034

[34] Dinis, P.B., Camotim, D.: A novel DSM-based approach for the rational design of fixed-ended and pin-ended short-to-intermediate thin-walled angle columns, Thin-Walled Struct, 87 (2015) 2, pp. 158-82, https://doi.org/10.1016/j.tws.2014.10.013

[35] Execution of steel structures and aluminium structures - Part 2: Technical requirements for steel structures EN 1090-2, Brussels, Belgium, CEN 2018.

[36] Eurocode 3: Design of steel structures - Part 1-5: Plated structural elements EN 1993-1-5, Brussels, Belgium, CEN 2006.

[37] Structural steel equal and unequal leg angles - Part 2: Tolerances on shape and dimensions. EN 10056-2, Brussels, Belgium, CEN 1998.

[38] ECCS. Manual on stability of steel structures. European Convention for Constructional Steelwork, 1976.

[39] Može, P., Cajot, L.G., Sinur, F., Rejec, K., Beg, D.: Residual stress distribution of large steel equal leg angles, Engineering Structures, 71 (2014), pp. 35-47, https://doi.org/10.1016/j.engstruct.2014.03.040

[40] Cruise, R.B., Gardner, L.: Residual stress analysis of structural stainless steel sections, J. Constr. Steel Res., 64 (2008), pp. 352-366, https://doi.org/10.1016/j.jcsr.2007.08.001

[41] Gardner, L., Cruise, R.: Modeling of residual stresses in structural stainless steel sections, J. Struct. Eng. ASCE 135 (2009) 1, pp. 42-53, https://doi.org/10.1061/(ASCE)0733-9445(2009)135:1(42)